光学学报

分布式光纤水听器技术研究和应用进展

王照勇[1,2*]，刘依凡[1,2]，陈义赐[1,2]，吴金懿[1,2]，陈柏琦[1,2]，高侃[1]，叶青[1,2]，蔡海文[1]

[1]中国科学院上海光学精密机械研究所空间激光信息传输与探测技术重点实验室，上海 201800；

[2]中国科学院大学材料与光电研究中心，北京 100049

摘要 分布式光纤水听器将光纤作为水下声波换能器阵列，是近年来发展的新型水听器技术，具有阵列灵活重构、易于大规模组网、湿端全自动制备等独特优势，得到了国内外相关领域的重点关注。介绍了分布式光纤水听器的基本传感原理与典型的信号解调方法，梳理了声压灵敏度、系统等效噪声、响应方向性、动态范围等分布式光纤水听器的重要性能指标与研究进展，并介绍了近年来分布式光纤水听器技术的应用概况。最后，对存在的问题与未来发展趋势进行了总结和展望。

关键词 分布式光纤水听器；分布式光纤声波传感；光纤传感；瑞利散射；水下目标探测

中图分类号 TN253；TN29 **文献标志码** A **DOI**：10.3788/AOS231627

1 引 言

声波探测是人类感知环境和信息交互的基本方式[1-3]，水听器技术是水下探测与通信的关键手段，在水下导航通信[4-6]、目标探测定位[7-8]、海洋资源勘探、海洋生态监测[9-10]等军民领域发挥着重要作用。目前，主流的水听器技术主要分为压电式水听器和光纤水听器[11-13]两大类。前者是利用压电效应实现声波探测的，已经得到了广泛应用；后者则主要利用光纤中激光特性（相位、频率、幅度等）对声压的响应来进行感知，具有探测灵敏度高、湿端无源、组网方便等优势，近几十年得到了迅猛发展和重点关注。然而，常规水听器为节点式探测，组阵规模受到复用技术的限制，通常难以实现超过一百阵元的大孔径阵列[14]；组阵后的阵元间距、阵列孔径等阵列参数固定，不能适应多样目标的探测需要；湿端部分需要手工制备，效率低下。现有水听器技术已经难以满足先进海洋科技和未来水声探测的严苛要求，如大规模探测阵列、快速灵活部署、自适应阵列重构、全天候长期观测、低成本大范围监测等，迫切需要发展一种全新的补充手段。

分布式光纤水听器（DFOH）技术是近年来发展的水声探测新技术[15]，该技术将光纤作为传感媒介，通过在光纤单端注入问询激光脉冲，定量获取光纤沿线各个位置的声波信息（幅度、频率、相位），从而将光纤转换为成千上万个声波换能器，具有空间密集感知、频率响应平坦、数字域阵列重构、可长距离大阵列探测（数十 km）等独特优势，有望满足先进水声探测的发展需要。此外，在工程应用方面，DFOH 的湿端可以全自动化制备，生产效率高、一致性好，满足大规模阵列建设和快速量产需要。2019 年，美国海军实验室公开表示，他们正在开展基于瑞利散射的新一代水听器技术的研究[16]。DFOH 技术开始得到相关领域的重点关注，近年来得到了蓬勃发展，其理论体系不断被优化，多方面性能得到了快速提升，应用场景迅速扩容。

当前，DFOH 技术尚处于起步发展阶段，仍然面临着诸多技术瓶颈和需要解决的难题，不断引起相关领域专家学者们的关注。本文对 DFOH 技术的水声探测原理和定量解调方法进行了梳理，整理了 DFOH 技术典型的性能指标概念与评价方法，总结了近年来的应用概况，并分析了可能的未来发展方向。

2 基本原理

2.1 DFOH 水声探测原理

DFOH 技术利用光纤所处声场对光纤内传输光波的调制作用将光纤转换为声波换能器，并通过光时域反射计（OTDR）或光频域反射计（OFDR）的方式对光纤不同位置的声波信息进行分离，进而实现光纤沿线声压的空间连续探测。假设光纤任一位置 z 所处声场的压强为 P_z，这一压强将引起光纤的径向应变

收稿日期：2023-10-08；**修回日期**：2023-10-27；**录用日期**：2023-11-06；**网络首发日期**：2023-11-17

基金项目：国家重点研发计划（2020YFC1522901）、中国科学院青年创新促进会人才项目（YIPA2023257）、上海市青年科技启明星计划项目（22QB1406000）

通信作者：*wzhy0101@siom.ac.cn

$e_z^r = P_z/Y$和轴向应变$e_z = \mu P_z/Y$，其中，Y和μ分别为光纤的杨氏模量与泊松比。根据弹光效应和胡克定律，光纤轴向应变将导致光纤内传输光波的时延与相位变化。经历光纤长度Δz后的累积相位变化$\Delta\phi_z$表示[17]为

$$\Delta\phi_z = (1+\gamma)n_0 k\Delta z e_z \approx 0.78 n_0 k\Delta z\,\mu P_z/Y, \quad (1)$$

式中：$\gamma = -0.22$为石英光纤的弹光系数；$n_0 \approx 1.5$为光纤纤芯折射率；$k = 2\pi/\lambda$为角波数（λ为波长）。显然，光波的相位变化$\Delta\phi_z$与声场的声压P_z呈线性映射关系，通过解调光波相位即可重建光纤沿线的声压信息。这一探测原理对于DFOH和干涉型光纤水听器来说是一致的，其区别在于DFOH的光波是入射光在光纤各个位置的后向瑞利散射，而干涉型光纤水听器的光波是入射光，这也正是DFOH可以实现空间连续声波探测的根本原因。

根据常规石英光纤的相关参数：$Y = 6.5\times10^{10}\ \mathrm{N/m^2}$、$\mu = 0.17$、$\lambda = 1550\ \mathrm{nm}$，当相位解调精度$\Delta\phi_z = 0.1\ \mathrm{rad}$时，裸光纤可实现的最小探测声压为

$$P = \frac{Y\Delta\phi_z}{(1+\gamma)n_0 k\mu\Delta z} \approx 806.2\ \mathrm{Pa}, \quad (2)$$

对应的声压级为$20\lg(P/10^{-6}) \approx 178\ \mathrm{dB}$，远大于零级海况的噪声水平（45 dB）。显然，这难以满足水声探测需要。为此，通常采用空心圆柱结构来提升光纤对声压的探测能力，如图1所示。在这一机制下，光纤的轴向应变由空心圆柱的结构参数和材料参数决定。声压P_z引起的外径形变量表示[18]为

$$\Delta a = \frac{P_z a}{Y_m}\cdot\left(\frac{a^2+b^2}{a^2-b^2} - \mu_m\right), \quad (3)$$

式中：a和b分别为空心圆柱的外半径和内半径；Y_m和μ_m分别为空心圆柱的杨氏模量和泊松比。考虑DFOH的光纤螺旋缠绕方式，假设光纤缠绕比为$\kappa = z_\delta/L_\delta = z/L$[其中，$L_\delta$为螺距，$z_\delta$为螺距对应的光纤长度，且满足$z_\delta^2 = (2\pi a)^2 + L_\delta^2$]，可以得到声压引起的光纤轴向应变：

$$e_{m,z} = \frac{\sqrt{[2\pi(a+\Delta a)]^2 + (1-\mu_m)^2 L_\delta^2} - \sqrt{(2\pi a)^2 + L_\delta^2}}{\sqrt{(2\pi a)^2 + L_\delta^2}} \approx \frac{4\pi^2 a\Delta a - \mu_m L_\delta^2}{(2\pi a)^2 + L_\delta^2}。 \quad (4)$$

光波经历光纤长度Δz后的累积相位变化更改为$\Delta\phi_{m,z} = (1+\gamma)n_0 k\Delta z e_{m,z}$。可见，此时光波相位变化对声压的响应主要取决于空心圆柱的结构参数（a、b）和材料参数（Y_m、μ_m）。光纤紧密缠绕情况下，$L_\delta \ll a$，$e_{m,z} \approx \Delta a/a$，以$a = 3.0\ \mathrm{cm}$、$b = 2.8\ \mathrm{cm}$的聚碳酸酯（PC）管为例，$Y_m = 2.38\ \mathrm{GPa}$，$\mu_m = 0.37$。当相位解调精度$\Delta\phi_{m,z} = 0.1\ \mathrm{rad}$时，可以计算得到该结构可实现的最小探测声压：

$$P_z = \frac{\Delta\phi_{m,z} Y_m}{(1+\gamma)n_0 k\Delta z\cdot\left(\frac{a^2+b^2}{a^2-b^2} - \mu_m\right)} \approx 0.355\ \mathrm{Pa}, \quad (5)$$

对应的声压级为$20\lg(P/10^{-6}) \approx 111\ \mathrm{dB}$。显然，光纤对声波的探测能力得到大幅提升（约67 dB）。如何优化相位解调精度以及提升光纤对声压的响应度成为DFOH在零级海况应用和安静型目标探测中面临的重要问题。

2.2　定量解调方法

DFOH是基于光纤后向瑞利散射进行声波探测的，其解调方法与干涉型光纤水听器有较大差异，需要对光纤各个位置的信息进行分离，以达到分布式空间多阵元探测的效果。1993年，Taylor等[19]提出了利用相干瑞利散射进行光纤沿线扰动定性监测的方法，并将其应用于周界安防[20]。2011年，中国科学院上海光学精密机械研究所团队[21]率先提出了基于数字相干相位解调的分布式定量测量方法，这标志着分布式光纤声波探测的首次实现。上海交通大学[22]、中国科学院半导体研究所[23]、南京大学[24]、英国南安普顿大学[25]、电子科技大学[26]、南方科技大学[27]等先后提出了各自的分布式定量测量方案，为DFOH奠定了坚实的基础。

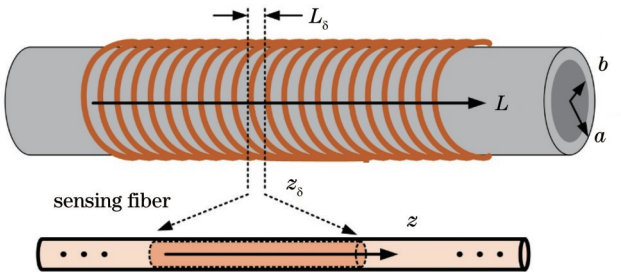

图1　空心圆柱结构与光纤增敏示意图

Fig. 1　Schematic diagram of hollow cylinder structure and optical fiber sensitization

DFOH的分布式定量解调主要分为相位解调和信道分离两部分，前者包括正交差分解调（数字域[21]、电学域、光学域[26]等）、相位生成载波解调（PGC）[23]、频移解调[28-29]等；后者则主要通过在数字域或光学域进行空间差分，结合OTDR或OFDR思想分离出光纤各个空间信道/阵元的探测信息，具体包括双脉冲方案[30-31]、延时自差方案[25,32]、频域映射[22]等。以正交相位解调和空间差分的相位敏感光时域反射计（Φ-OTDR）方案[21]为例，如图2所示。假设问询光波为理想单频激光脉冲$\tilde{E}_{in} = E_0\mathrm{rect}\left(t_z/\tau\right)\exp\left[\mathrm{j}(\omega+\Delta\omega)t_z + \mathrm{j}\varphi_0\right]$，其中，$E_0$是光电场幅度，$\omega$是光波中心角

频率，$\Delta\omega$是声光调制器引入的频移，φ_0是初始相位，τ是脉冲宽度，t_z是光波在光纤中的往返传输时间，$t_z=2n_0z/c$（c为真空中的光速）。光波在光纤任一位置z的后向散射光返回后表示为

$$\tilde{E}_{\mathrm{back}}(z)=E_{\mathrm{back}}\exp\left(\mathrm{j}\phi_{\mathrm{back}}\right)=E_0\exp\left[-2\alpha z-\mathrm{j}(\omega+\Delta\omega)t_z\right]r_{\mathrm{c}}(z)\cdot\exp\left[\mathrm{j}\int_0^z 2\beta(\xi)\mathrm{d}\xi\right],\tag{6}$$

式中：$r_{\mathrm{c}}(z)$是整个光脉冲在位置z处的综合瑞利散射系数[33]，与瑞利散射和多波束干涉有关；E_{back}、ϕ_{back}分别是后向散射光的幅度和相位；$\exp(-\alpha z)$是传输损耗；$\beta(\xi)$是传输常数。散射光与本振光发生干涉，耦合器的一路输出光强信号为

$$P=\left|\tilde{E}_0\exp(\mathrm{j}\omega t_z+\mathrm{j}\varphi_0)+\mathrm{j}\tilde{E}_{\mathrm{back}}(z)\right|^2=E_0^2+E_{\mathrm{back}}^2+2E_0E_{\mathrm{back}}\cos\left\{\Delta\omega t_z+\exp\left[\mathrm{j}\int_0^z 2\beta(\xi)\mathrm{d}\xi\right]\right\},\tag{7}$$

在差分作用下，双平衡探测器输出表示为$i_{\mathrm{AC}}\propto 4E_0E_{\mathrm{back}}\cos\left\{\Delta\omega t_z+\exp\left[\mathrm{j}\int_0^z 2\beta(\xi)\mathrm{d}\xi\right]\right\}$。根据数字相位解调方法思想，散射光的相位信息的计算公式为

$$\phi_z=\int_0^z 2\beta(\xi)\mathrm{d}\xi=\mathrm{angle}\left[\int i_{\mathrm{AC}}\exp(\Delta\omega t')\mathrm{d}t'\right]+2k\pi,\ k=0,\pm1,\pm2,\cdots,\tag{8}$$

式中，angle(·)表示求取相位信息。进一步地，通过空间差分可以得到光波经过光纤长度Δz后的累积相位变化$\Delta\phi_z=\phi_{z+\Delta z}-\phi_z=\int_z^{z+\Delta z}\beta(\xi)\mathrm{d}\xi$。结合上述相关理论，即可获得裸光纤或增敏结构周边的声压信息，从而实现声压探测。

在频移方案中，利用扫频光源对光波的时延特性进行表征，结合互相关[29,34]等方法获取时延信息，以此映射光纤轴向应变情况，实现外界声压的定量探测。

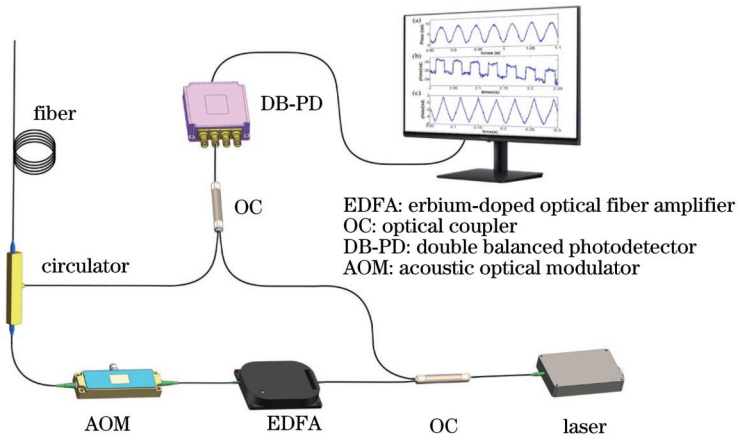

图 2　基于相位解调与空间差分的 Φ-OTDR 系统

Fig. 2　Φ-OTDR system with phase demodulation and spatial difference

3　性能指标与发展概况

随着DFOH的不断发展，人们逐步认识到这一技术与常规光纤水听器技术的共性与差异，建立了针对DFOH的性能表征和量化评估体系。

3.1　响应度/声压灵敏度

响应度定义为每单位声压强所产生的相位变化，即$M_{\mathrm{p}}=\partial\varphi/\partial P$，用于表征DFOH探测信号对外界声压的响应系数，又称声压灵敏度。响应度的量纲为rad/Pa，通常采用指数级进行量化评估，即$M=20\lg(M_{\mathrm{P}}/M_{\mathrm{r}})$，其中，$M_{\mathrm{r}}=1\ \mathrm{rad}/\mu\mathrm{Pa}$是参考灵敏度。DFOH的声压灵敏度测试原理与干涉型光纤水听器基本相同，测试方法包括驻波管法、自由场测试法等（GB/T 42559—2023）。需要注意的是，DFOH各个阵元具有不可忽视的探测孔径，测试时需要确保整个探测孔径的光纤/增敏结构处于同一声波波前，以保障测试结果的准确性；自由场测试时应考虑球面波的扩散作用并对其进行校正。

根据式(1)可知，一段长度$\Delta z=10\ \mathrm{m}$裸光纤的声压灵敏度约为$M_{\mathrm{p}}=(1+\gamma)n_0k\mu\Delta z/Y$，代入石英光纤的相关参数可得，$M_{\mathrm{p}}\approx1.24\times10^{-10}\ \mathrm{rad}/\mu\mathrm{Pa}$（约$-198\ \mathrm{dB}$），类似地，可以计算出每米裸光纤的声压灵敏度约为$-208\ \mathrm{dB}$。根据式(5)，空心圆柱结构光纤的声压灵敏度表示为

$$M_{\mathrm{p}}=(1+\gamma)n_0k\cdot\frac{\Delta z}{Y_m}\cdot\left(\frac{a^2+b^2}{a^2-b^2}-\mu_{\mathrm{m}}\right)。\tag{9}$$

可以看出，空心圆柱结构光纤的声压灵敏度受到结构参数和材料参数的影响较大。以图1所示结构为例，其声压灵敏度为$2.819\times10^{-7}\ \mathrm{rad}/\mu\mathrm{Pa}$，约为$-131\ \mathrm{dB}$，较裸光纤提升67 dB。需要说明的是，上述两个表达式[式(1)、(5)]表示了裸光纤和声敏光缆的声压灵敏度，尚未考虑DFOH探测孔径内的积分作

用与光波往返经过扰动区的影响。

DFOH的声压灵敏度主要由传感光纤和增敏结构决定，代表性声压灵敏度如表1所示。需要说明的是，常规干涉型光纤水听器的声压灵敏度一般在－140 dB re rad/μPa左右[35]，部分研究性成果可以高达－120 dB re rad/μPa左右[36]，压电水听器的声压灵敏度在－190 dB re V/μPa量级[35]。

表1 代表性DFOH声压灵敏度

Table 1 Representative sound pressure sensitivity of DFOH

Year	Group	Responsivity (re rad/μPa)	Outer diameter / mm	Bearable pressure	Method
2015	Laser Institute, Shandong Academy of Sciences[37]	－158.0 dB	—	—	Ultra-weak fiber grating array (UWFBG)
2016	Beihang University[38]	－150.0 dB	—	—	PGC demodulation method and optimizing the path difference and pulse width
2017	ITMO National Research University[39]	－169.4 dB @ 495 Hz; －143.7 dB @ 40 Hz	＜20.0	—	UWFBG, secondary coating of strong polymer fiber and thermoplastic rubber outer sheath (material is RTV655, Y_m = 5.6 MPa, thickness is 3.5 mm)
2018	Institute of Semiconductors, Chinese Academy of Sciences (CAS)[40]	－141.6 dB @ (20-1000) Hz	12.5	—	Hollow cylindrical structure probe based on elastic sensitive material, μ_m = 0.4, Y_m = 32 MPa
2020	Zhejiang Lab[41]	－131.0 dB @ (1-1024) Hz	—	—	Acoustic sensitive optical cable formed by spiral winding of optical fiber in elastic material
2021	Huazhong University of Science and Technology[42]	－127.0 dB @ (100-2000) Hz	20.0	—	UV exposure scattering enhancement point, spiral winding structure of the optical cable, winding ratio is 1∶5, elastic material Y_m = 10 MPa, sound-transparent sheath
2021	Shanghai Institute of Optics and Fine Mechanics (SIOM), CAS[43]	－146.0 dB @ (20-500) Hz	12.5	Not lower than 3 MPa; lateral pressure is not less than 10 N/mm	Spiral winding structure of the optical cable, winding ratio is 1∶7.5, elastic material μ_m = 0.4, Y_m = 1.1 GPa, Polyurethane sheath
2022	Zhejiang Lab[44]	－130.0 dB @ (4-700)Hz	—	—	Node type towed array optical cable, optical fiber spiral winding
2023	Huazhong University of Science and Technology[45]	－137.2 dB @ (5-2000) Hz; －125.3 dB @ 1 Hz	22.0	0.3 MPa, pulling force is 47.5 kN	Scattering enhancement point, optical fiber spiral winding, elastic material μ_m = 0.35, Y_m = 400 MPa

3.2 系统噪声水平/灵敏度

系统噪声水平(NL)是一种用于表征单位频率内DFOH干端系统噪声功率分布情况的概率统计指标。一般通过系统噪声$\phi_n(t)$的功率谱密度(PSD)或其均方根来表征NL，表达式为$\Phi_{\mathrm{PSD}}(f)=\lim\limits_{T\to\infty}\sum\left|\phi_n(f)\right|^2\Big/T=\int_{-\infty}^{\infty}R(t)\mathrm{e}^{-\mathrm{j}2\pi ft}\mathrm{d}t$或$\Phi_{\mathrm{PSD,s}}(f)=\sqrt{\lim\limits_{T\to\infty}\sum\left|\phi_n(f)\right|^2\Big/T}$，其中，$\sum(\cdot)$表示累加函数，$T$是噪声统计时长，$R(t)$是系统噪声的自相关函数，$\phi(f)$是系统噪声的频域表征。DFOH系统的NL可以直接利用解调的相位信号进行评估，量纲为$\mathrm{rad^2/Hz}$或$\mathrm{rad}\Big/\sqrt{\mathrm{Hz}}$，又称相位解调噪声、灵敏度[46-49]；也可以转换为轴向应变进行评估，$\Phi_{\mathrm{PSD},\varepsilon}(f)=\Phi_{\mathrm{PSD}}(f)\Big/\left[2(1+\gamma)n_0k\Delta z\right]^2$，量纲为$\varepsilon^2/\mathrm{Hz}$或$\varepsilon\Big/\sqrt{\mathrm{Hz}}$。以裸光纤为例，差分距离$\Delta z$ = 10 m，1 p$\varepsilon\Big/\sqrt{\mathrm{Hz}}$对应94.8 μrad$\Big/\sqrt{\mathrm{Hz}}$。NL的指数级为$20\lg\Phi_{\mathrm{PSD,s}}(f)=10\lg\Phi_{\mathrm{PSD}}(f)$。一般将传感光纤放置于安静环境(隔振箱、静音室等)中，利用光纤尾端的解调信号对DFOH

系统NL进行评估测试。需要注意的是，频率间隔、脉冲重复频率、数据窗长度等参数对PSD的幅度数值有较大影响，在测试中需要进行规范化处理。

受限于微弱的瑞利散射系数（等效反射率约为－70 dB/m），DFOH系统的NL偏高。在国内外同行的共同努力下，散射增强、分集探测等多类技术得以提出并实现，DFOH系统NL得到不断优化，如表2所示。

表2 代表性DFOH NL

Table 2 Representative NL of DFOH

Year	Group	System NL	Method
2018	Institute of Semiconductors, CAS[50]	900 $\mu rad/\sqrt{Hz}$	Active optical fiber
2018	Paris-Saclay University Nokia Bell Labs[51]	10 $\mu rad/\sqrt{Hz}$	PDM-QPSK (polarization division multiplexing quadrature phase shift keting) coding, polarization division coherent detection, 10 UWFBGs
2018	Universidad de Alcalá[52]	4 $p\varepsilon/\sqrt{Hz}$	SOA (semiconductor optical amplifier) amplification, DWDM (dense wavelength division multiplexing) filtering, high-speed sampling (10 GS/s)
2019	Wuhan University of Technology[53]	2239 $\mu rad/\sqrt{Hz}$	UWFBG, a new method based on 3×3 coupler demodulation and PGC demodulation
2019	Universidad de Alcalá[54]	5 $p\varepsilon/\sqrt{Hz}$	Chirped pulse Φ-OTDR, post-processing interpolation method
2019	Paris-Saclay University Nokia Bell Labs[55]	－30 dB@25.1 km, －50 dB@0.1 km	Polarization diversity BPSK (binary phase shift keying) coding
2019	Shanghai Jiao Tong University [56]	220 $p\varepsilon/\sqrt{Hz}$@108 km	TGD-OFDR (time-gated digital optical frequency domain reflectometry), bidirectional distributed Raman amplification, hamming window query pulse
2020	United States Naval Research Laboratory[57]	－91 dB re $rad/\sqrt{Hz}$	Fiber scattering enhancement point based on femtosecond laser
2020	SIOM, CAS[58]	－67.8 dB re $rad/\sqrt{Hz}$	5-level frequency diversity and 4-level wavelength diversity
2021	SIOM, CAS[59]	－70 dB re $rad/\sqrt{Hz}$	Dense multichannel signal integration
2022	Wuhan University of Technology[60]	－50.2 dB; 58.3 $p\varepsilon/\sqrt{Hz}$	UWFBG array, inserting-zero Gray code coding
2022	SIOM, CAS[61]	－88 dB re $rad/\sqrt{Hz}$; 0.15 $p\varepsilon/\sqrt{Hz}$	Fiber transverse mode diversity and frequency diversity

3.3 系统等效噪声

系统等效噪声（NE）指DFOH系统整体（含干端设备和湿端光缆）的噪声功率谱分布情况，一般用于表征DFOH进行水声探测能够有效感知的最小声压，又常称作系统自噪声。系统NEN_{DFOH}是由干端设备的系统NLΦ_{PSD}和湿端光缆的声压灵敏度M_p共同决定的，$N_{DFOH}=\Phi_{PSD}/M_p$，量纲为$\mu Pa/\sqrt{Hz}$。系统NE的指数级为$N_e=20\lg(N_{DFOH}/N_r)$，其中，$N_r=1\ \mu Pa/\sqrt{Hz}$是参考等效噪声。干涉型光纤水听器的NE一般为28～50 dB[35]，压电陶瓷水听器的NE一般为32～65 dB[36]。

目前，针对DFOH系统NE的研究还较少。2017年，Lavrov等[39]利用UWFBG阵列构成反射单元，利用RTV655材料对其进行二次涂覆，制备了外径为20 mm的湿端光缆，结合PGC解调技术，实验中系统NE达到53.0 mPa/$\sqrt{Hz}$@495 Hz、8.3 mPa/$\sqrt{Hz}$@40 Hz，约为94.5 dB、78.4 dB。2023年，华中科技大学孙琪真教授团队[45]通过在弹性材料上螺旋缠绕刻有散射增强点的光纤构建了湿端光缆，结合外差分偏振探测技术，将系统NE降至48 dB@1 kHz，达到零级海况噪声水平（45～50 dB），有望实现极安静型目标的探测。

3.4 动态范围

动态范围是系统可检测的最大信号与最小信号的

比值，表示为 $R_{\mathrm{D}}=20\lg\left(\Delta\phi_{\max}/\Delta\phi_{\min}\right)$，用于评估DFOH在嘈杂环境下对弱信号的探测能力，量纲为dB。在DFOH中，最小可检测信号一般受限于系统$\mathrm{NL}\Phi_{\mathrm{PSD}}(f)$，最大检测信号则与系统解调方法有关。在相位解调方案中，最大检测信号主要受限于相位的卷绕特性，时域相邻两点信号之间的差异不能超过π。考虑单频信号的最大斜率绝对值为1，频率为f_{a}的声波信号可有效检测的最大值$\Delta\phi_{\max}$满足$2\Delta\phi_{\max}\sin(\pi f_{\mathrm{a}}/f_{\mathrm{s}})\leqslant\pi$，其中，$f_{\mathrm{s}}$是问询光脉冲的重复频率，可以得到动态范围$R_{\mathrm{D}}=20\lg(\Delta\phi_{\max})-\Phi_{\mathrm{PSD}}(f)$。在频移解调方案中，动态范围会受到光源扫频范围和系统采样带宽的限制，较大扫描范围可以满足较大信号的检测需要，但解调精度较低，反之亦然。

DFOH的动态范围的研究还相对较少。2021年，华中科技大学Fan等[62]提出了一种“微分-解卷绕-积分”(DUI)的相位解卷绕方法，实现了较大信号的有效检测，将最大检测信号提升至1043 rad，动态范围达到131.7 dB@1.08 kHz。2022年，中山大学Wu等[63]利用时间差分和加权测量方法成功实现了幅度为2.367 με、频率为200 Hz的信号重建，将最大检测信号的幅度提升100.1倍。相信在国内外同行的共同努力下，DFOH动态范围会得到快速提升。

3.5　响应方向性/指向性

响应方向性用于表征DFOH系统对不同方向入射声波的响应能力，又称指向性。不同于常规点式水听器，DFOH各个阵元具有不可忽视的探测孔径[64-66]，阵元输出是探测孔径内声场的积分结果，具有独特的阵元响应方向性。

在近场[67]情况，如图3(a)所示，光纤位置z处声场分布表示为$\tilde{E}_{\mathrm{a}}(r_z,t)=(E_{\mathrm{a}}/r_z)\cdot\exp(\mathrm{j}w_{\mathrm{a}}t)$，其中，$t$为时间，$E_{\mathrm{a}}$为声场幅度，$w_{\mathrm{a}}$为声波角频率，$r_z$是声源与DFOH任一阵元的间距。根据DFOH传感原理可以得到阵元信号，表示为

$$\Delta\phi_z(r_z,\theta)=E_{\mathrm{a}}g_z\exp(\mathrm{j}w_{\mathrm{a}}t)\cdot\int_z^{z+\Delta z}\frac{\exp\left[-\mathrm{j}k_{\mathrm{a}}\sqrt{r_z^2+(\xi-z)^2/\kappa^2-2r_z(\xi-z)\sin\theta/\kappa}\right]}{\sqrt{r_z^2+(\xi-z)^2/\kappa^2-2r_z(\xi-z)\sin\theta/\kappa}}\mathrm{d}\xi,\tag{10}$$

式中：$k_{\mathrm{a}}=2\pi f_{\mathrm{a}}/v_{\mathrm{a}}$是声波的传播常数($v_{\mathrm{a}}$是声波传输速度)；$\kappa$是声敏光缆的缠绕比；$g_z$是阵元响应系数。因此，可以得到指向性响应，即

$$M_\theta=\exp(\mathrm{j}w_{\mathrm{a}}t)\cdot\int_z^{z+\Delta z}\frac{\exp\left[-\mathrm{j}k_{\mathrm{a}}\sqrt{r_z^2+(\xi-z)^2/\kappa^2-2r_z(\xi-z)\sin\theta/\kappa}\right]}{\sqrt{r_z^2+(\xi-z)^2/\kappa^2-2r_z(\xi-z)\sin\theta/\kappa}}\mathrm{d}\xi。\tag{11}$$

在远场[67]情况，如图3(b)所示，声场分布表示为$\tilde{E}_{\mathrm{a}}(r,t)=E_{\mathrm{a}}\exp(\mathrm{j}w_{\mathrm{a}}t+k_{\mathrm{a}}r)$，阵元信号为$\Delta\phi_z(\theta)=E_{\mathrm{a}}g_z\exp(\mathrm{j}w_{\mathrm{a}}t)\cdot\int_z^{z+\Delta z}\exp\left[\mathrm{j}k_{\mathrm{a}}(\xi-z)\sin\theta/\kappa\right]\mathrm{d}\xi$，指向性响应为

$$M_\theta=\exp(\mathrm{j}w_{\mathrm{a}}t)\cdot\int_z^{z+\Delta z}\exp\left[\mathrm{j}k_{\mathrm{a}}(\xi-z)\sin\theta/\kappa\right]\mathrm{d}\xi=\frac{2\kappa\sin(k_{\mathrm{a}}\Delta z\sin\theta/2\kappa)}{k_{\mathrm{a}}\sin\theta}\cdot\exp(\mathrm{j}w_{\mathrm{a}}t+\mathrm{j}k_{\mathrm{a}}\Delta z\sin\theta/2\kappa)。\tag{12}$$

可见，DFOH的指向性与常规水听器具有非常大的差异[68]，受到声波频率、探测孔径、光纤缠绕比等多种因素的影响，需要根据使用场景进行合理选择和布设。

3.6　讨　　论

除了上述几项，DFOH还有诸多性能评价指标，如频响范围、信道间串扰、输出稳定性、一致性等，相关理论大多与常规光纤水听器[69]的定义一致，此处不作赘述。需要说明的是，由于DFOH的大探测孔径和空间积分作用，加之各类分集技术与高空间分辨率技术[61,70]等，其信道间串扰较常规水听器更复杂，尚未见到DFOH信道间串扰成熟理论的相关报道。

此外，为了便于相关领域学者对DFOH性能进行更为充分的了解和对比，梳理了基于DFOH的简易声呐系统的有效探测距离指标。这一指标受到系统等效噪声N_{DFOH}、水文环境(环境背景噪声级S_{am}、声波传输

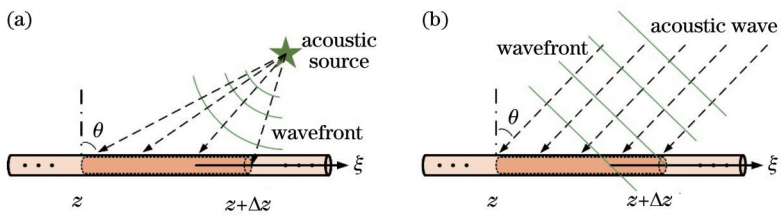

图3　DFOH阵元的指向性模型。(a)近场；(b)远场

Fig. 3　Directivity models of DFOH array. (a) Near field; (b) far field

衰减 α_L)、待测目标特性(目标声源级 S_{SPL}、声波频率 f)、水声信号处理方法(系统增益 G)等多方面因素的影响。对于特定声波频率 f 的待测目标,有效探测距离 L 满足约束条件

$$S_{\mathrm{SPL}}-\alpha_L+G-S_{\mathrm{am}}-N_{\mathrm{DFOH}}>D_{\mathrm{th}}, \tag{13}$$

式中:声源级 S_{SPL} 是距离声源 1 m 处声强相对于参考声强 I_0 的分贝数,$S_{\mathrm{SPL}}=10\lg(I/I_0)$,声强 $I=P^2/\rho_{\mathrm{a}}\upsilon_{\mathrm{a}}$,其中,$\rho_{\mathrm{a}}$、$\upsilon_{\mathrm{a}}$ 分别是水的密度和声波传输速度;传输衰减主要包括球面波扩散作用和声波传输损耗,表示为 $\alpha_L=20\lg(L)+\alpha L$,吸收系数的经验公式为 $\alpha(f)=0.102f^2/(1+f^2)+40.7f^2/(4100+f^2)+3.06\times10^{-4}f^2$,量纲为 dB/km;系统增益是指利用各个阵元的探测信息进行有效融合[59]所实现的探测增益,同理也可以是单个阵元在时间域的冗余信息进行融合所实现的增益,两者所带来的增益提升与阵元数量 N、积分时间 T、有效带宽 B 有关,$G=10\lg(N)+5\lg(B\cdot T)$;$D_{\mathrm{th}}$ 是有效探测阈值,一般取 3 dB,在水听器领域,有时为了获取较好的目标定位性能,D_{th} 也会取 12 dB。

以 $N_{\mathrm{DFOH}}=50$ dB(NL 为 −75 dB、$M_{\mathrm{p}}=-125$ dB)的 DFOH 系统为例,考虑不同目标的有效探测距离如表 3 所示。

表 3 不同目标的 DFOH 声呐的有效探测距离[71]

Table 3 Effective detection range of DHOH sonar for various targets[71]

Target type	Sound source level /dB	Effective detection range /km
High noise submarine	>165	>47
Noise submarine	145-165	35-47
Quiet submarine	125-145	23-35
Extremely quiet submarine	<125	<23

Notes: (i) The count of array elements $N=50$ for spatial gain, the time-average gain is negelected, the source frequency is 10 Hz and $D_{\mathrm{th}}=3$ dB; (ii) the results are obtained in ideal model, and the practical performance will be influenced by factors in actual applications, including hydrologic condition, sound features of targets, etc.

4 应用情况进展

DFOH 具有可大规模组网、阵列灵活重构、湿端全自动制备等独特优势,近年来得到了国内外水声探测领域的广泛关注。2015 年,山东省科学院激光研究所[37]率先利用自差延时解调的 Φ-OTDR 系统与 UWFBG 阵列串构成 DFOH 系统,并在实验室水箱中对系统的水声探测能力进行了可行性验证,其声压灵敏度为 −158 dB,相位噪声为 −56 dB。2017 年,Lavrov 等[39]同样采用自差延时解调 Φ-OTDR,将 4 组 UWFBG 制备成声敏光缆,首次在开阔水域对 DFOH 的水声探测能力进行了验证,其最高声压灵敏度达到 −143 dB,系统 NE 为 8.3 mPa/$\sqrt{\mathrm{Hz}}$,动态范围为 70 dB。随后,中国科学院半导体研究所与湖南大学联合团队[40]、之江实验室等[41]利用驻波管法对 DOFH 的水声探测能力进行了验证,其声压灵敏度分别达到 −141.6 dB 和 −131.0 dB。2021 年,中国科学院上海光学精密机械研究所[43]报道了 DFOH 的第一次湖试结果,确认了 DFOH 的实用性能,如图 4 所示。至此,DFOH 的水声探测能力与实用性能得到了充分验证,近年来在水下目标探测、海底地震波监测等领域得到了快速发展。

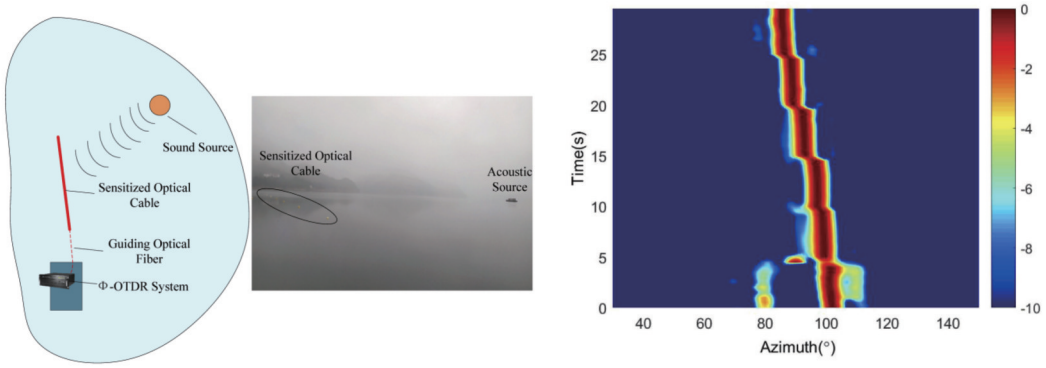

图 4 第一次湖试试验布设与目标定向结果[43]

Fig. 4 Experimental layout and target direction result in the first lake test[43]

4.1 悬浮水平阵

随着主动降噪、消声瓦等舰艇降噪技术的不断发展,极安静型潜艇的自噪声已经达到甚至低于海洋背景噪声的水平,但其低频段噪声仍然难以下降,而且低频段声波(100 Hz 以下)在水中的传播衰减小,传输距离远,如何有效探测目标低频段噪声并实现定位/定向

成为水听器技术面临的一项重要难题。悬浮水平阵通过锚绳和浮子将水听器阵列固定于水中或海底，可以方便地构建大规模孔径阵列，满足各类水下/水面目标的探测定位需要。得益于长探测距离和空间密集感知特性，DFOH技术可以充分发挥悬浮水平阵的优势，在数字域灵活构建阵列，同时满足近场高频目标定位和远场低频目标定向的需要，因此近年来这一方向得到了重点关注。

2018年起，国内外开始针对DFOH的空间多维定位技术开展研究[65,72]。2019年，中国科学院上海光学精密机械研究所相关研究团队[65]率先分析了DFOH独特的空间积分响应，首次建立了DFOH分布式阵列模型，如图5所示，将测量标距（gauge length，$z_{i-2,1}^{(f)}-z_{i-2,0}^{(f)}$）对应的空间跨度定义为阵元孔径，相邻信道的起始位置间隔（$z_{i-1,0}-z_{i-2,0}$）定义为阵元间距，并对这一模型独特存在的阵元交叠（overlap）现象进行了说明；利用阵列信号处理方法在空气中实现了DFOH空间二维和三维定位探测。随后，中国科学院上海光学精密机械研究所[43]报道了利用声敏光缆构建悬浮水平阵进行目标定向的结果。同期，上海大学相关研究团队[73]提出了基于到达时间差（TDOA）的多维定位方法。接着，中国人民解放军海军工程大学相关研究团队[74]在浅水区域利用悬浮水平阵实现了最大25 m距离的目标定位。相关研究证实，DFOH具备构建悬浮水平阵的能力，可以实现水下目标的有效探测和定位跟踪，为DFOH的岸基部署奠定了前期基础。

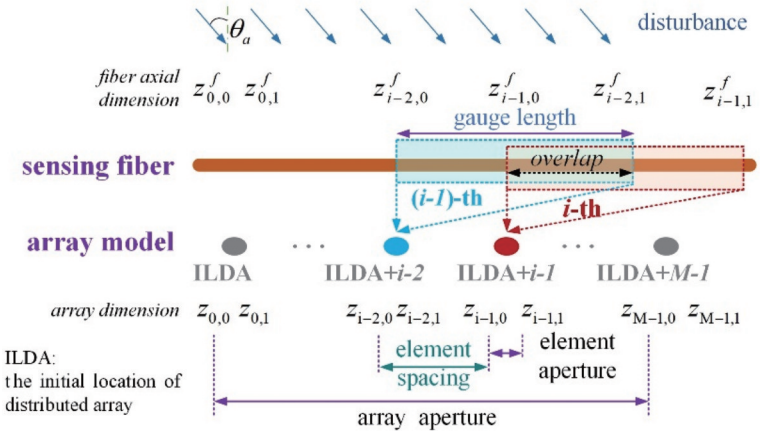

图5 DFOH分布式阵列模型[65,75]

Fig. 5 Distributed array model of DFOH[65,75]

4.2 轻量化拖曳阵

拖曳式线性水听阵，简称拖曳阵，是20世纪70年代研制的一种声呐阵列[76]，如美国的战术线列阵声呐系统STASS、海狼级潜艇的TB-16D与TB-12X、TB-29A等[77]，可以方便地布放于舰艇、水下潜航器（UUV）、飞机等平台，充分利用水文条件，机动灵活地实现局部海域的快速探测与持续监测。相较于舰基、艇基声呐，拖曳阵的长度受拖曳平台尺寸的限制较小[78]，更易于构建大孔径阵列，探测范围更大，更易于实现低频段、静音型目标的探测，而且其探测阵列与拖曳载具的距离远，受拖曳载具的影响小，工作环境更佳。DFOH所需光缆的内部结构单一，无干涉臂，无须波分复用器件等，仅需螺旋缠绕增敏或涂覆增敏，更易于实现轻量化，且外径更小，极大地降低了拖曳阵对平台的存储空间要求和拖曳动力要求，满足更大探测孔径、更大探测范围和更低频段的探测需要，而且可以方便地部署于无人载具，实现更为灵活的远程机动监测，有望成为现有水下探测的重要补充手段。

目前，DFOH拖曳阵的相关研究报道较少。2021年，中国人民解放军海军工程大学相关研究团队[79]率先提出了这一应用方向，利用涂覆增敏和弱反射光栅（WFBG）形成了束管式拖曳线阵，其外径仅为1.7 mm，声压灵敏度达到−139 dB，此外，他们理论分析了拖曳的流噪声情况。随后，之江实验室相关研究团队[44]于2023年利用螺旋缠绕的节点式增敏探头形成拖曳阵，以此降低流噪声和信道串扰，在2～3级海况下开展了DOFH的第一次海试，对流噪声（图6）、模拟声源进行了探测验证。这两项研究工作初步验证了DFOH拖曳阵的技术可行性，对其流噪声有了初步定量化的认识。DFOH拖曳阵尚处于起步阶段，还面临诸多挑战，如流噪声控制、低频段探测能力提升、干端设备轻量化等，但有理由相信，DFOH拖曳阵未来将充分发挥空间密集感知、阵列灵活可重构、轻量化等独特优势，满足特定场景对低性能、小型化、低成本拖曳阵的快速布放需求，得到目标探测领域的重点关注。

4.3 通信海缆声波阵

DFOH不仅可以利用特种光缆实现水下声波信号的探测，也可以将海底通信光缆转换为海洋声波与地震波的换能器阵列[80-82]，满足水下目标探测、海洋灾害监测[82-84]、海洋地球物理[85-88]、油气资源勘探、海洋生态监测等领域的需要。该技术可以直接将现有的海底通信光缆作为传感阵列，充分利用遍布全球海底的冗

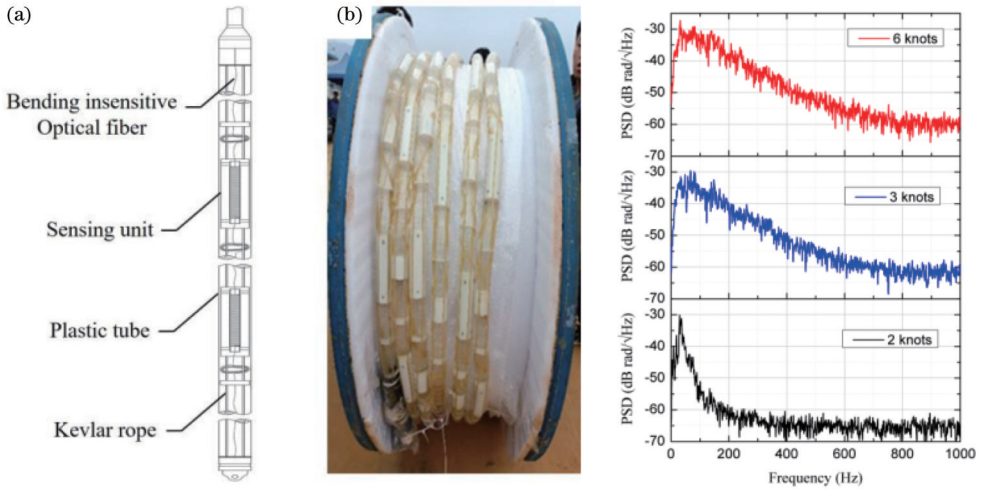

图 6 节点式 DFOH 拖曳缆结构、实物样品与流噪声测试结果[44]

Fig. 6 Cable structure, sample and its flow noise of the nodal DFOH towing cable[44]

余通信光纤，应用成本极低，监测范围大，而且采样时空密度高，具有前所未有的发展潜力。

基于通信海缆的 DFOH 已经在地震波探测方面得到了广泛的关注和发展[80,89]，在水声探测方面的研究较少，相关研究团队中，挪威科技大学、美国康奈尔大学等形成的联合团队最具代表性。2022 年，该团队[90]报道了首次基于海底通信光缆的海洋野生动物声波探测研究，利用北极长度为 120 km 的海底通信光缆实现了须鲸叫声的有效探测和鲸鱼分布密度估算；之后实现了鲸鱼、船只等目标的探测[91]，为海洋动物预测、船舶跟踪、船舶防撞等提供了一种实时监测网络；2023 年，该团队[92]利用近乎平行的两条长度为 260 km 的海底光缆实现了 8 只长须鲸长达 5 h 的定位与轨迹跟踪，监测距离达到 800 km，气枪试验显示，定位误差约为 100 m，如图 7 所示。先驱者的研究确定了基于 DFOH 与海底通信光缆的水声探测的可行性，并探索验证了其对鲸鱼、船只等目标的探测与定位能力，有望为广阔海域目标探测、海洋生态健康监测、海底资源被动勘探等提供一种全新的低成本、高密度、全天候实时监测手段，这将改变相关领域的游戏规则，发展潜力巨大。

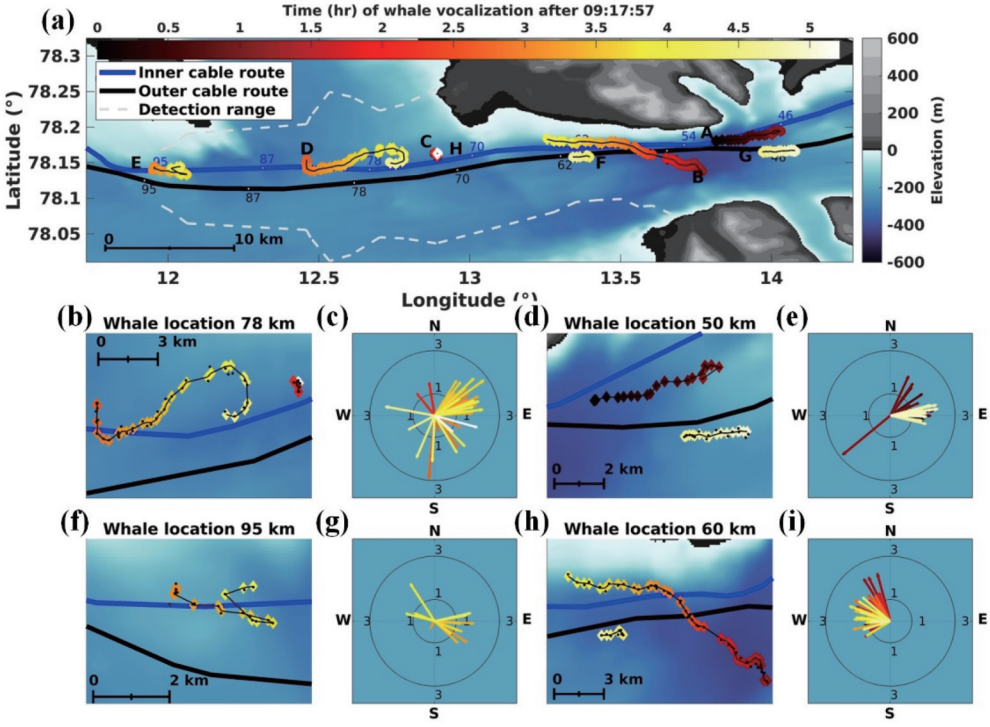

图 7 利用北极海底光缆进行多头鲸鱼的同时定位跟踪[92]。(a)长度为 60 km 的电缆截面概览；(b)～(i)不同位置的鲸鱼轨迹以及对应的鲸鱼的移动速度

Fig. 7 Simultaneously tracking of multiple whales with submarine communication cable in the Arctic[92]. (a) Overview of 60 km communication cable; (b)-(i) whale traces at different positions and corresponding swim speeds of whales

5 展 望

DFOH在水声探测与目标定位领域尚处于初步研究阶段，目前还存在诸多问题亟待解决，部分关键性能指标还没有得到充分研究，尚未建立较为完备的理论体系。DFOH具有独特的空间积分响应，信道间扰动与常规点式水听器存在较大差异，大规模阵列技术对信道间串扰的要求高，目前尚未见到相关研究报道；大多已有研究集中在DFOH干端设备技术与湿端光缆设计，对DFOH干湿端整体的研究较少，动态范围、系统NE等指标还有待进一步提升。但是，DFOH的应用发展潜力巨大。更低的系统自噪声、多分量探测、指向性侦听[75]等更强的探测能力将满足更多的应用场景需要；得益于湿端光缆的轻量化优势，干端设备的小型化、轻量化、低功耗等研究[93-94]将极大推动DFOH在小型无人载具拖曳阵的快速应用，有利于利用海缆中继站实现覆盖全球海域范围的目标检测与生态监测，实现海洋声波的“观测云平台”[91]；DFOH具有长距离、空间连续感知、易于大规模组网的独特优势，可以方便地构建水平阵、垂直阵、阵列集群等多样性探测阵列，也可方便地构建大规模主动定位系统，满足目标检测、水下导航、海洋通信等领域的需求。

6 结束语

DFOH作为一种新兴的水声探测手段，具有空间连续感知、阵列灵活重构、湿端全自动制备、低成本、轻量化等独特优势，发展迅猛、潜力巨大，已经在悬浮水平阵、轻量化拖曳阵、通信海缆声波阵等应用场景得到了验证。围绕DFOH的基本探测原理、关键技术指标、代表性应用场景进行了重点介绍，并对存在的问题和可能的发展方向进行评述。我们相信，DFOH必将在水下目标探测、海洋通信导航、环境生态健康等领域发挥重要作用，成为一项不可或缺的技术手段。

参 考 文 献

[1] Hopwood F L. Submarine acoustics[J]. Nature, 1919, 103(2598): 467-469.

[2] Duarte C M, Chapuis L, Collin S P, et al. The soundscape of the anthropocene ocean[J]. Science, 2021, 371(6529): eaba4658.

[3] Carl W. Advance in global ocean acoustics[J]. Science, 2020, 369(6510): 1433-1434.

[4] Katzschmann R K, DelPreto J, MacCurdy R, et al. Exploration of underwater life with an acoustically controlled soft robotic fish [J]. Science Robotics, 2018, 3(16): eaar3449.

[5] Afzal S S, Akbar W, Rodriguez O, et al. Battery-free wireless imaging of underwater environments[J]. Nature Communications, 2022, 13: 5546.

[6] Jin P, Fu J, Wang F L, et al. A flexible, stretchable system for simultaneous acoustic energy transfer and communication[J]. Science Advances, 2021, 7(40): eabg2507.

[7] Tian S Z, Chen D B, Wang H, et al. Deep convolution stack for waveform in underwater acoustic target recognition[J]. Scientific Reports, 2021, 11: 9614.

[8] Toky A, Singh R P, Das S. Localization schemes for underwater acoustic sensor networks: a review[J]. Computer Science Review, 2020, 37: 100241.

[9] Madsen P T, Siebert U, Elemans C P H. Toothed whales use distinct vocal registers for echolocation and communication[J]. Science, 2023, 379(6635): 928-933.

[10] Matoza R S, Fee D, Assink J D, et al. Atmospheric waves and global seismoacoustic observations of the January 2022 Hunga eruption, Tonga[J]. Science, 2022, 377(6601): 95-100.

[11] Bucaro J A, Dardy H D, Carome E F. Optical fiber acoustic sensor[J]. Applied Optics, 1977, 16(7): 1761-1762.

[12] 畅楠琪, 黄晓砥, 王海斌. 基于EKF参数估计的光纤水听器PGC解调方法研究[J]. 中国激光, 2022, 49(17): 1709001.
Chang N Q, Huang X D, Wang H B. Phase generated carrier demodulation approach in fiber-optic hydrophone based on extended kalman filter parameter estimation[J]. Chinese Journal of Lasers, 2022, 49(17): 1709001.

[13] 胡琪浩, 朱小谦, 马丽娜, 等. 无源干涉型光纤布拉格光栅水听器研究进展[J]. 激光与光电子学进展, 2023, 60(11): 1106015.
Hu Q H, Zhu X Q, Ma L N, et al. Advances in passive-interferometric type fiber Bragg grating-based hydrophones[J]. Laser & Optoelectronics Progress, 2023, 60(11): 1106015.

[14] 孟洲, 陈伟, 王建飞, 等. 光纤水听器技术的研究进展[J]. 激光与光电子学进展, 2021, 58(13): 1306009.
Meng Z, Chen W, Wang J F, et al. Research progress of fiber optic hydrophone technology[J]. Laser & Optoelectronics Progress, 2021, 58(13): 1306009.

[15] 苑立波, 童维军, 江山, 等. 我国光纤传感技术发展路线图[J]. 光学学报, 2022, 42(1): 0100001.
Yuan L B, Tong W J, Jiang S, et al. Road map of fiber optic sensor technology in China[J]. Acta Optica Sinica, 2022, 42(1): 0100001.

[16] Dandridge A. Fiber optic interferometric sensors at sea[J]. Optics and Photonics News, 2019, 30(6): 34-41.

[17] Fang Z J, Chin K K, Qu R H, et al. Fundamentals of optical fiber sensors[M]. Weinheim: Wiley, 2012.

[18] Murray M J, Davis A, Redding B. Fiber-wrapped mandrel microphone for low-noise acoustic measurements[J]. Journal of Lightwave Technology, 2018, 36(16): 3205-3210.

[19] Taylor H F, Lee C E. Apparatus and method for fiber optic intrusion sensing: US5194847[P]. 1993-03-16.

[20] Juarez J C, Maier E W, Choi K N, et al. Distributed fiber-optic intrusion sensor system[J]. Journal of Lightwave Technology, 2005, 23(6): 2081-2087.

[21] Pan Z Q, Liang K Z, Ye Q, et al. Phase-sensitive OTDR system based on digital coherent detection[J]. Proceedings of SPIE, 2011, 8311: 83110S.

[22] Liu Q W, Fan X Y, He Z Y. Time-gated digital optical frequency domain reflectometry with 1.6-m spatial resolution over entire 110-km range[J]. Optics Express, 2015, 23(20): 25988-25995.

[23] Fang G S, Xu T W, Feng S W, et al. Phase-sensitive optical time domain reflectometer based on phase-generated carrier algorithm[J]. Journal of Lightwave Technology, 2015, 33(13): 2811-2816.

[24] Tu G J, Zhang X P, Zhang Y X, et al. The development of an Φ-OTDR system for quantitative vibration measurement[J]. IEEE Photonics Technology Letters, 2015, 27(12): 1349-1352.

[25] Masoudi A, Newson T P. High spatial resolution distributed optical fiber dynamic strain sensor with enhanced frequency and strain resolution[J]. Optics Letters, 2017, 42(2): 290-293.

[26] Wang Z N, Zhang L, Wang S, et al. Coherent Φ-OTDR based on I/Q demodulation and homodyne detection[J]. Optics Express, 2016, 24(2): 853-858.

[27] Liu S Q, Yu F H, Xu W J, et al. Direct demodulation of differential phase from Φ-OTDR using self-homodyne phase diversity receiver[C]//2021 Asia Communications and Photonics

Conference (ACP), October 24-27, 2021, Shanghai, China. New York: IEEE Press, 2022.
[28] Pastor-Graells J, Martins H F, Garcia-Ruiz A, et al. Single-shot distributed temperature and strain tracking using direct detection phase-sensitive OTDR with chirped pulses[J]. Optics Express, 2016, 24(12): 13121-13133.
[29] Qiu L Q, Ba D X, Zhou D W, et al. High-sensitivity dynamic distributed pressure sensing with frequency-scanning φ-OTDR [J]. Optics Letters, 2022, 47(4): 965-968.
[30] Sha Z, Feng H, Zeng Z M. Phase demodulation method in phase-sensitive OTDR without coherent detection[J]. Optics Express, 2017, 25(5): 4831-4844.
[31] He X G, Xie S R, Liu F, et al. Multi-event waveform-retrieved distributed optical fiber acoustic sensor using dual-pulse heterodyne phase-sensitive OTDR[J]. Optics Letters, 2017, 42 (3): 442.
[32] Shang Y, Yang Y H, Wang C, et al. Optical fiber distributed acoustic sensing based on the self-interference of Rayleigh backscattering[J]. Measurement, 2016, 79: 222-227.
[33] Zhou J, Pan Z Q, Ye Q, et al. Characteristics and explanations of interference fading of a Φ-OTDR with a multi-frequency source[J]. Journal of Lightwave Technology, 2013, 31(17): 2947-2954.
[34] Fernández-Ruiz M R, Costa L, Martins H F. Distributed acoustic sensing using chirped-pulse phase-sensitive OTDR technology[J]. Sensors, 2019, 19(20): 4368.
[35] Plotnikov M Y, Lavrov V S, Dmitraschenko P Y, et al. Thin cable fiber-optic hydrophone array for passive acoustic surveillance applications[J]. IEEE Sensors Journal, 2019, 19(9): 3376-3382.
[36] 周宏坤. 航空声纳浮标用矢量水听器及其悬挂技术研究[D]. 哈尔滨: 哈尔滨工程大学, 2016: 19-60.
Zhou H K. Research on vector hydrophone for aerial sonar buoy and its suspension technology[D]. Harbin: Harbin Engineering University, 2016: 19-60.
[37] Wang C, Shang Y, Liu X H, et al. Distributed OTDR-interferometric sensing network with identical ultra-weak fiber Bragg gratings[J]. Optics Express, 2015, 23(22): 29038-29046.
[38] Shang Y, Yang Y H, Wang C, et al. Study on demodulated signal distribution and acoustic pressure phase sensitivity of a self-interfered distributed acoustic sensing system[J]. Measurement Science and Technology, 2016, 27(6): 065201.
[39] Lavrov V S, Plotnikov M Y, Aksarin S M, et al. Experimental investigation of the thin fiber-optic hydrophone array based on fiber Bragg gratings[J]. Optical Fiber Technology, 2017, 34: 47-51.
[40] Yang Y, Xu T W, Feng S W, et al. Optical fiber hydrophone based on distributed acoustic sensing[J]. Proceedings of SPIE, 2018, 10849: 108490B.
[41] Guan H J, Han B, Han Z W, et al. High performance DAS-based optical fiber hydrophone[C]//Asia Communications and Photonics Conference/International Conference on Information Photonics and Optical Communications 2020 (ACP/IPOC), October 24-27, 2020, Beijing, China. Washington, DC: Optica Publishing Group, 2020: M4A.100.
[42] Chen J F, Li H, Liu T, et al. Fully distributed hydroacoustic sensing based on lightweight optical cable assisted with scattering enhanced fiber[C]//2021 Optical Fiber Communications Conference and Exhibition (OFC), June 6-10, 2021, San Francisco, CA, USA. New York: IEEE Press, 2021.
[43] Lu B, Wu B Y, Gu J F, et al. Distributed optical fiber hydrophone based on Φ-OTDR and its field test[J]. Optics Express, 2021, 29(3): 3147-3162.
[44] Yan G F, Long J Q, Jiang L, et al. High performance marine towing cable system based on ultra-sensitive fiber-optic distributed acoustic sensing[C]//2022 Asia Communications and Photonics Conference (ACP), November 5-8, 2022, Shenzhen, China. New York: IEEE Press, 2023: 174-177.
[45] Chen J F, Li H, Xiao X P, et al. Fully distributed hydroacoustic sensing based on ultra-highly sensitive and lightweight fiber-optic hydrophone cable[J]. Optics and Lasers in Engineering, 2023, 169: 107734.
[46] Gabai H, Eyal A. On the sensitivity of distributed acoustic sensing[J]. Optics Letters, 2016, 41(24): 5648-5651.
[47] Gabai H, Eyal A. How to specify and measure sensitivity in distributed acoustic sensing (DAS)? [J]. Proceedings of SPIE, 2017, 10323: 103238A.
[48] Alekseev A E, Tezadov Y A, Potapov V T. Sensitivity of a phase-sensitive optical time-domain reflectometer with a semiconductor laser source[J]. Laser Physics, 2018, 28(6): 065105.
[49] Wang Z Y, Lu B, Ye Q, et al. Recent progress in distributed fiber acoustic sensing with Φ-OTDR[J]. Sensors, 2020, 20(22): 6594.
[50] Feng S W, Xu T W, Huang J F, et al. Enhanced SNR phase-sensitive OTDR system with active fiber[J]. Proceedings of SPIE, 2018, 10849: 108490C.
[51] Dorize C, Awwad E. Enhancing the performance of coherent OTDR systems with polarization diversity complementary codes [J]. Optics Express, 2018, 26(10): 12878-12890.
[52] Costa L, Martins H F, Martin-Lopez S, et al. Reaching p$\varepsilon/\sqrt{\mathrm{Hz}}$ sensitivity in a distributed optical fiber strain sensor [C]//26th International Conference on Optical Fiber Sensors, September 24-28, 2018, Lausanne, Switzerland. Washington, DC: OSA, 2018: TuD3.
[53] Zhou C M, Pang Y D, Qian L, et al. Demodulation of a hydroacoustic sensor array of fiber interferometers based on ultra-weak fiber Bragg grating reflectors using a self-referencing signal [J]. Journal of Lightwave Technology, 2019, 37(11): 2568-2576.
[54] Costa L, Martins H F, Martín-López S, et al. Fully distributed optical fiber strain sensor with 10^{-12} $\varepsilon/\sqrt{\mathrm{Hz}}$ sensitivity[J]. Journal of Lightwave Technology, 2019, 37(18): 4487-4495.
[55] Dorize C, Awwad E, Renaudier J. High sensitivity Φ-OTDR over long distance with polarization multiplexed codes[J]. IEEE Photonics Technology Letters, 2019, 31(20): 1654-1657.
[56] Chen D, Liu Q W, He Z Y. 108-km distributed acoustic sensor with 220-p$\varepsilon/\sqrt{\mathrm{Hz}}$ strain resolution and 5-m spatial resolution[J]. Journal of Lightwave Technology, 2019, 37(18): 4462-4468.
[57] Redding B, Murray M J, Donko A, et al. Low-noise distributed acoustic sensing using enhanced backscattering fiber with ultra-low-loss point reflectors[J]. Optics Express, 2020, 28(10): 14638-14647.
[58] Gu J F, Lu B, Yang J Q, et al. High SNR Φ-OTDR based on frequency and wavelength diversity with differential vector aggregation method[J]. IEEE Photonics Journal, 2020, 12(6): 7103612.
[59] Wang Z Y, Yang J Q, Gu J F, et al. Practical performance enhancement of DAS by using dense multichannel signal integration[J]. Journal of Lightwave Technology, 2021, 39(19): 6348-6354.
[60] Tang J G, Wang G D, Lü W H, et al. Distributed acoustic sensing system based on inserting-zero Golay coding with ultra-weak fiber Bragg gratings[J]. IEEE Sensors Journal, 2022, 22 (16): 15985-15990.
[61] Lu B, Gu J F, Wang Z Y, et al. Ultra-low-noise MIMO distributed acoustic sensor using few-mode optical fibers[J]. Journal of Lightwave Technology, 2022, 40(9): 3062-3071.
[62] Fan C Z, Li H, He T, et al. Large dynamic range optical fiber distributed acoustic sensing (DAS) with differential-unwrapping-integral algorithm[J]. Journal of Lightwave Technology, 2021, 39(22): 7274-7280.
[63] Wu Y C, Cao Z H, Zhang S Q, et al. Dynamic range

enlargement of distributed acoustic sensing based on temporal differential and weighted-gauge approach[J]. Journal of Lightwave Technology, 2022, 40(9): 3038-3045.

[64] Li W M, Lu Y, Chen Y, et al. Directivity research of sensing channels in a distributed fiber optic hydrophone[J]. Journal of Physics: Conference Series, 2023, 2486(1): 012082.

[65] Liang J J, Wang Z Y, Lu B, et al. Distributed acoustic sensing for 2D and 3D acoustic source localization[J]. Optics Letters, 2019, 44(7): 1690-1693.

[66] 杨竣淇, 王照勇, 刘依凡, 等. 基于相位校正的分布式光纤大探测孔径多维定位[J/OL]. 中国激光: 1-15[2023-06-20]. http://kns.cnki.net/kcms/detail/31.1339.tn.20231114.1006.026.html.
Yang J Q, Wang Z Y, Liu Y F, et al. Multi-dimensional positioning of distributed optical fiber with large probe aperture in phase correction[J/OL]. Chinese Journal of Laser: 1-15[2023-06-20]. http://kns. cnki. net/kcms/detail/31.1339.tn.20231114.1006.026.html.

[67] Mailloux R J. Phased array antenna handbook[M]. 2nd ed. Boston: Artech House, 2005.

[68] Li W M, Chen Y, Liang Y, et al. Directivity dependence of a distributed fiber optic hydrophone on array structure[J]. Sensors, 2022, 22(16): 6297.

[69] 黄俊斌, 宋文章, 顾宏灿, 等. 分布反馈式光纤激光水听器探头封装及应用研究进展[J]. 激光与光电子学进展, 2023, 60(1): 0100002.
Huang J B, Song W Z, Gu H C, et al. Research progress on packaging and application of distributed feedback fiber laser hydrophone probe[J]. Laser & Optoelectronics Progress, 2023, 60(1): 0100002.

[70] Lu B, Pan Z Q, Wang Z Y, et al. High spatial resolution phase-sensitive optical time domain reflectometer with a frequency-swept pulse[J]. Optics Letters, 2017, 42(3): 391-394.

[71] 高学强, 杨日杰. 潜艇辐射噪声声源级经验公式修正[J]. 声学与电子工程, 2007, 3: 17-18, 21.
Gao X Q, Yang R J. Modification of empirical formula for sound source level of submarine radiated noise[J]. Acoustics and Electronics Engineering, 2007, 3: 17-18, 21.

[72] Shpalensky N, Shiloh L, Gabai H, et al. Use of distributed acoustic sensing for Doppler tracking of moving sources[J]. Optics Express, 2018, 26(13): 17690-17696.

[73] Liu Z C, Zhang L, Wei H M, et al. Underwater acoustic source localization based on phase-sensitive optical time domain reflectometry[J]. Optics Express, 2021, 29(9): 12880-12892.

[74] Cao W H, Cheng G L, Xing G X, et al. Near-field target localisation based on the distributed acoustic sensing optical fibre in shallow water[J]. Optical Fiber Technology, 2023, 75: 103198.

[75] Wang Z Y, Yang J Q, Gu J F, et al. Multi-source aliasing suppression for distributed fiber acoustic sensing with directionally coherent enhancement technology[J]. Optics Letters, 2020, 45(20): 5672-5675.

[76] Lemon S G. Towed-array history, 1917-2003[J]. IEEE Journal of Oceanic Engineering, 2004, 29(2): 365-373.

[77] 刘孟庵. 拖曳线列阵声呐技术发展综述[J]. 声学与电子工程, 2006, 3: 1-5.
Liu M A. Review on the development of towed linear array sonar technology[J]. Acoustics and Electronics Engineering, 2006, 3: 1-5.

[78] 张春雷. 用于拖曳阵的矢量水听器研究[D]. 哈尔滨: 哈尔滨工程大学, 2011.
Zhang C L. Research on vector hydrophone for towed array[D]. Harbin: Harbin Engineering University, 2011.

[79] 丁朋, 黄俊斌, 庞彦东, 等. 弱反射光纤光栅水听器拖曳线列阵[J]. 光子学报, 2021, 50(7): 0706004.
Ding P, Huang J B, Pang Y D, et al. A towed line array with weak fiber Bragg grating hydrophones[J]. Acta Photonica Sinica, 2021, 50(7): 0706004.

[80] 王照勇, 卢斌, 叶蕾, 等. 分布式光纤声波传感及其地震波检测应用[J]. 激光与光电子学进展, 2021, 58(13): 1306006.
Wang Z Y, Lu B, Ye L, et al. Distributed optical fiber acoustic sensing and its application to seismic wave monitoring[J]. Laser & Optoelectronics Progress, 2021, 58(13): 1306006.

[81] Li J X, Kim T, Lapusta N, et al. The break of earthquake asperities imaged by distributed acoustic sensing[J]. Nature, 2023, 620(7975): 800-806.

[82] Taweesintananon K, Landrø M, Potter J R, et al. Distributed acoustic sensing of ocean-bottom seismo-acoustics and distant storms: a case study from Svalbard, Norway[J]. Geophysics, 2023, 88(3): B135-B150.

[83] Jousset P, Currenti G, Schwarz B, et al. Fibre optic distributed acoustic sensing of volcanic events[J]. Nature Communications, 2022, 13: 1753.

[84] Wilcock W. Illuminating tremors in the deep[J]. Science, 2021, 371(6532): 882-884.

[85] Cheng F, Chi B X, Lindsey N J, et al. Utilizing distributed acoustic sensing and ocean bottom fiber optic cables for submarine structural characterization[J]. Scientific Reports, 2021, 11: 5613.

[86] Lior I, Rivet D, Ampuero J P, et al. Magnitude estimation and ground motion prediction to harness fiber optic distributed acoustic sensing for earthquake early warning[J]. Scientific Reports, 2023, 13: 424.

[87] Lindsey N J, Dawe T C, Ajo-Franklin J B. Illuminating seafloor faults and ocean dynamics with dark fiber distributed acoustic sensing[J]. Science, 2019, 366(6469): 1103-1107.

[88] Sladen A, Rivet D, Ampuero J P, et al. Distributed sensing of earthquakes and ocean-solid Earth interactions on seafloor telecom cables[J]. Nature Communications, 2019, 10: 5777.

[89] Matsumoto H, Araki E, Kimura T, et al. Detection of hydroacoustic signals on a fiber-optic submarine cable[J]. Scientific Reports, 2021, 11: 2797.

[90] Bouffaut L, Taweesintananon K, Kriesell H J, et al. Eavesdropping at the speed of light: distributed acoustic sensing of baleen whales in the Arctic[J]. Frontiers in Marine Science, 2022, 9: 901348.

[91] Landrø M, Bouffaut L, Kriesell H J, et al. Sensing whales, storms, ships and earthquakes using an Arctic fibre optic cable [J]. Scientific Reports, 2022, 12: 19226.

[92] Rørstadbotnen R A, Eidsvik J, Bouffaut L, et al. Simultaneous tracking of multiple whales using two fiber-optic cables in the Arctic[J]. Frontiers in Marine Science, 2023, 10: 1130898.

[93] Liu Y, Yang J, Wang Z, et al. High performance miniaturized DAS-based hydrophone with spatial deviation method and marine object detection[C]// 28th International conference on Optical Fiber Sensors (OFS), November 20-24, 2023, ACT CITY, Hamamatsu, Japan. Tu3.35.

[94] Xu T W, Ma L L, Yang K H, et al. Mini-distributed acoustic sensing module for submarine application[J]. Optical Engineering, 2021, 60(3): 034106.

Research and Application Progress of Distributed Fiber Optic Hydrophone Technology

Wang Zhaoyong[1,2*], Liu Yifan[1,2], Chen Yici[1,2], Wu Jinyi[1,2], Chen Baiqi[1,2], Gao Kan[1], Ye Qing[1,2], Cai Haiwen[1]

[1]*Key Laboratory of Space Laser Communication and Detection Technology, Shanghai Institute of Optics and Fine Mechanics, Chinese Academy of Sciences, Shanghai* 201800, *China*;

[2]*Center of Materials Science and Optoelectronics Engineering, University of Chinese Academy of Sciences, Beijing* 100049, *China*

Abstract

Significance Acoustic detection is a basic way for human beings to perceive the environment. Hydrophone technologies are key means of underwater acoustic detection and play an important role in target detection, communication, navigation, resource exploration, and marine ecological monitoring. At present, the mainstream hydrophone technologies are mainly divided into two categories of piezoelectric hydrophone and fiber optic hydrophone (FOH). The former has been widely applied, and FOH rapidly developing in recent decades features high detection sensitivity, unpowered wet-end, and convenient networking. However, these conventional hydrophones have many disadvantages. First, they are in nodal type, the multiplexing scale and array size are limited, and the largest array number is far less than 1000. Second, their array parameters (array spacing, array aperture, etc.) cannot be changed after being determined, and the target type to be located is limited, which cannot meet the detection needs of various targets. Finally, the wet-end part needs to be prepared by hand due to the complex fiber connect relationship. Therefore, the existing hydrophone technologies are difficult to meet the strict requirements of advanced marine science and future underwater acoustic detection, such as large-scale detection arrays, rapid and flexible deployment, adaptive array reconstruction, and low-cost large-scale monitoring. Meanwhile, it is extremely important to develop new hydrophone technologies.

Distributed fiber optic hydrophone (DFOH) technology is a new underwater acoustic detection technology developed in recent years. In DFOH, the optical fiber is converted into thousands of acoustic transducers, and all acoustic information can be obtained along the fiber quantitatively and spatial-continuously from the backscattering of the inquiry laser pulse. DFOH has unique advantages including densely spatial sensing, flat frequency response, flexible array reconstruction in the digital domain, and large array (tens of kilometers). Additionally, in terms of engineering applications, the wet-end of DFOH can be mechanically produced with high efficiency and good consistency, which is essential on large-scale array construction and rapid mass production. In 2019, the Naval Research Laboratory in the United State publicly stated that research was being conducted on a new generation of hydrophone technology based on Rayleigh scattering, and afterward, DFOH technology attracted widespread attention and was rapidly developed.

Progress In DFOH, the sensing fiber is converted into acoustic transducers by utilizing the laser phase response to the external sound field, and the external sound field is continuously detected in the spatio-temporal domain, with each channel separated in the way of optical time domain reflectometer (OTDR) or optical frequency domain reflectometer (OFDR). Thus, the fundamental principle is divided into laser phase response and signal demodulation. On the former, the DFOH response mechanism is consistent with that of conventional interferometric FOH, and fiber secondary coating and wed-end structured design (Fig. 1) are also effective in improving the DFOH response (sound pressure sensitivity). On signal demodulation, DFOH is quite different from FOH and channel separating is essential, with complex backscattering mixing along the fiber. The principle details are introduced by us.

The DFOH performance has been rapidly enhanced in recent decades. The preliminary foundation of DFOH is built from phase-sensitive OTDR. The first qualitative demodulation was proposed by Taylor in 1993, and the first quantitative demodulation (Fig. 2) was realized by the Shanghai Institute of Optics and Fine Mechanics (SIOM), Chinese Academy of Sciences in 2011. Soon afterward, many demodulation methods are proposed. The DFOH concept was first proposed in 2015, when the Shandong Academy of Sciences verified the feasibility of DFOH to detect underwater sound in the laboratory, with sound pressure sensitivity of −158 dB and phase noise of −56 dB. With the joint efforts of domestic and foreign scholars, the DFOH performance indexes are greatly improved, including sound pressure sensitivity (Table 1), system noise level (Table 2), system equivalent noise, dynamic range, and response directivity (Fig. 3). Meanwhile, the effective detection range (Table 3) of DFOH passive sonar system is theoretically evaluated, and the evaluation system of DFOH performance is gradually improved.

In recent years, the dry-end technology and wet-end cables keep optimizing, laboratory tests constantly improve, and the applications are explored in underwater suspended horizontal array, lightweight towed array, and hydrophone array with submarine communication cables. On the underwater suspended horizontal array, direction and localization of underwater target and lake tests are focused, and the representative groups are from SIOM (Figs. 4 and 5), Shanghai University, and Naval University of Engineering. The lightweight towing array application is still in the exploratory stage, the flow noise and channel crosstalk are studied, and Naval University of Engineering and Zhejiang Laboratory (Fig. 6) are the most representative groups. In terms of hydrophone array with submarine communication cables, the joint team of the Norwegian University of Science and Technology and Cornell University is the biggest concern, and they detect and track whales in the Arctic with existing submarine cables (Fig. 7), which is expected to provide a new means of all-weather monitoring for target detection in vast sea areas.

Conclusions and Prospects As a novel hydrophone technology, DFOH has unique advantages of continuous spatial detection, flexible array reconstruction, automatable wet-end production, light weight, and low cost. In recent years, DFOH has developed rapidly and has been verified in many application scenarios. We introduce the basic sensing principle and typical demodulation methods of DFOH and review the important performance indexes and research progress, including sound pressure sensitivity, system equivalent noise, response directivity, and dynamic range. Some representative applications are also introduced, such as underwater suspended horizontal array, lightweight towed array, and hydrophone array with submarine communication cables. Additionally, the existing problems and possible development trends are discussed. We believe that DFOH will play an important role in underwater target detection, marine communication and navigation, and environmental ecological monitoring.

Key words distributed fiber optic hydrophone; distributed optical fiber acoustic sensing; optical fiber sensing; Rayleigh scattering; underwater target detection